A comprehensive study of reported high-metallicity giant H II regions – II. Ionizing stellar populations

Marcelo Castellanos,[1]★ Angeles I. Díaz[1] and Elena Terlevich[2]†

[1]*Departamento de Física Teórica, C-XI, Universidad Autónoma de Madrid, 28049 Madrid, Spain*
[2]*INAOE, Tonantzintla, Apdo. Postal 51, 72000 Puebla, México*

ABSTRACT

The ionizing stellar populations of 11 H II regions in the spiral galaxies: NGC 628, 925, 1232 and 1637, all of them reported to have solar or oversolar abundances according to empirical calibrations, have been analysed using stellar population synthesis models.

Four of the observed regions in the sample show features which indicate the presence of a population of Wolf–Rayet (WR) stars with ages between 2.3 and 4.1 Myr. This population is sufficient to explain the emission line spectrum of the low-metallicity region H13 in NGC 628, taking into account the uncertainties involved in both observations and model computations. This is not the case for the rest of the regions for which a second ionizing population is required to simultaneously reproduce both the WR features and the emission line spectrum. Composite populations are also found for half of the regions without WR features, although in this case, the result is based only on the emission line spectrum analysis.

For two of the regions showing WR features, no consistent solution is found, as the population containing WR stars produces a spectral energy distribution which is too hard to explain the emission of the gas. Several solutions are proposed to solve this problem.

Key words: stars: Wolf–Rayet – H II regions – galaxies: abundances – galaxies: stellar content.

1 INTRODUCTION

Metallicity affects stellar evolution in at least two different ways: by increasing the opacity of the stellar material and through the strengthening of the wind-driven mass-loss in high-mass stars. The former implies a lower effective temperature for the atmospheres of ionizing stars of higher metal content even at zero age, while the latter can severely affect the evolution of the most massive stars, leading, in the most extreme cases, to the almost complete loss of their outer envelopes.

The first of these effects should be readily observable as an inverse correlation between the metallicity and the temperature of the ionizing radiation for H II regions of different metallicities. In fact, there is a general agreement about the hardening of the ionizing radiation in regions of low metal content (e.g. Campbell, Terlevich & Melnick 1986; Cerviño & Mas-Hesse 1994). The inverse situation, however (i.e. the softening of the ionizing radiation in regions of high metal content), is more difficult to establish because, in these cases, the determination of both metal abundance and ionizing temperature is rather difficult. For the first one we have to rely, in general, on uncertain semi-empirical calibrations when the involved abundances are higher than about 1/2 solar. For the second one, there are no suitable

nebular emission line diagnostics. Recently, Bresolin, Kennicutt & Garnett (1999) have investigated a possible relation between ionizing stellar temperature and metallicity in giant H II regions in spiral galaxies through the use of the softness parameter η' (Vílchez & Pagel 1988), concluding that their results are consistent with a significant decrease in mean stellar temperatures of the ionizing stars with increasing metallicity. This decrease, however, is difficult to quantify, because in this work the metallicity is derived from the abundance parameter R_{23} (Pagel et al. 1979) and both η' and R_{23} depend to some extent on the degree of ionization of the nebula (Díaz et al. 1991). On the other hand, the method can be applied to a large number of H II regions and therefore can provide trends statistically significant.

A different approach consists of deriving the metal abundance from the direct determination of the electron temperature in the nebula and the ionizing temperature from the fitting of single star photoionization models. The method requires both high-quality spectroscopy and detailed modelling. In a previous paper (Díaz et al. 2000a, hereafter DCTG00) we have applied this procedure to H II regions in the spiral galaxy NGC 4258. The combination of these data with similar ones in the literature also seems to point to a decrease of mean ionizing temperature with increasing metallicity. Surprisingly, this is so even in the presence of Wolf–Rayet (WR) stars.

The presence of these stars provides an additional constraint to characterize the ionizing stellar population. In the last few years,

★E-mail: marcelo.castellanos@uam.es
†Visiting Fellow, IoA, Cambridge.

stellar evolution models for massive stars, taking into account mass-loss at different metallicities, have been calculated in order to reproduce the observed features of WR stars. The model predictions are however quite different depending on the assumed mass loss. In fact, models that assume a standard mass loss rate underpredict the number of galactic WR stars in comparison with observations (Maeder & Meynet 1994) while an enhanced mass-loss rate fits most WR population properties except for the mass loss rate itself (Leitherer, Chapman & Koribalski 1997). Therefore, the detailed observation and modelling of giant H II regions showing WR features can help to shed some light on this very important issue.

It would also be desirable to check the hardening of the ionizing radiation due to the presence of Wolf–Rayet stars predicted on theoretical grounds (Pérez 1997). These stars are supposed to change drastically the spectral energy distribution of an ionizing star cluster at energies higher than ∼40 eV. Models predict that this change depends both on the age and the metallicity of the burst (Schaerer & Vacca 1998, hereafter SV98) and, as a result of this, ionic elemental ratios are expected to change as well as ion-weighted temperatures.

A puzzling result in DCTG00 was the relatively low effective temperatures found in the two ionizing clusters with WR features, suggesting that either the rate of high energy photons is lower than expected or that the opacity in WR envelopes is highly efficient. This matter can be investigated through the observation of WR features in high metallicity H II regions where the effect of the mass loss rate on the effective temperature of the ionizing stars is supposed to be most enhanced.

In order to analyse the effects of metallicity on both stellar evolution and ionizing radiation, we have analysed a sample of reported high-metallicity H II regions by combining evolutionary synthesis models for ionizing populations and photoionization models in a self-consistent way. In this paper a detailed analysis of the ionizing populations of the observed regions is presented.

2 PHYSICAL PROPERTIES OF THE OBSERVED H II REGIONS

The observations of the sample H II regions analysed here – four in NGC 628, two in NGC 925, four in NGC 1232 and one in NGC 1637 – are described in detail in (Castellanos, Díaz & Terlevich 2002, hereafter Paper I) and consist of spectrophotometry in the 4000–9700 Å range. These data were complemented with those by van Zee et al. (1998) in order to provide a complete set of emission line ratios in the spectral range from 3500 to 9700 Å. For every region the physical conditions of the ionized gas – particle density, electron temperatures, ionic and total abundances – and functional parameters – ionization parameter and temperature of the ionizing radiation – as derived from the application of single star photoionization models were determined and are summarized in Table 1 for the regions analysed here.

For each of them we have calculated the Hα luminosity, $L(\text{H}\alpha)$, the number of hydrogen ionizing photons, $Q(\text{H})$, the angular effective diameter, ϕ, the filling factor, ϵ, the mass of ionized hydrogen, $M(\text{H II})$, and the mass content in the ionizing clusters, M^*. These quantities have been derived according to the expressions given in Díaz (1998), for our adopted distances: 7.3 Mpc for NGC 628, 8.6 Mpc for NGC 925, 21.5 Mpc for NGC 1232 and 7.8 Mpc for NGC 1637 (see Paper I) and are listed in Table 2.

Table 1. Summary of derived gas physical conditions of the analysed H II regions.

Galaxy	Region	n_e	$t(\text{S}^{++})$	$t(\text{N}^+)$	$\langle t \rangle_{\text{adopt}}$	$12 + \log(\text{O/H})$	$\log(\text{N/O})$	$\log(\text{S/O})$	$\log U$	T_{eff} (K)
NGC 628	H13	80	1.02 ± 0.03	0.90 ± 0.06	–	8.24 ± 0.08	-1.08 ± 0.04	-1.83 ± 0.04	-2.78 ± 0.10	35000
	H3	$\leqslant 40$	1.03 ± 0.05	–	–	8.23 ± 0.15	-1.14 ± 0.10	-1.85 ± 0.11	-2.92 ± 0.15	36000
	H4	$\leqslant 40$	0.95 ± 0.05	–	–	8.31 ± 0.15	-0.97 ± 0.10	-1.80 ± 0.11	-2.95 ± 0.15	35000
	H5	$\leqslant 40$	0.82 ± 0.06	–	–	8.34 ± 0.15	-1.07 ± 0.10	-1.67 ± 0.10	-2.97 ± 0.15	34800
NGC 925	CDT1	$\leqslant 40$	–	–	0.86	8.52	-1.07	-1.83	-3.00 ± 0.30	36500
	CDT4	$\leqslant 40$	–	–	0.93	8.41	-1.01	-1.83	-3.00 ± 0.25	36000
NGC 1232	CDT1	130	0.54 ± 0.05	0.67 ± 0.05	–	8.95 ± 0.20	-0.81 ± 0.08	-1.81 ± 0.10	-2.95 ± 0.20	34900
	CDT2	$\leqslant 40$	–	–	0.81	8.61 ± 0.15	-1.15 ± 0.10	-1.81 ± 0.15	-2.95 ± 0.15	36900
	CDT3	223	0.74 ± 0.05	0.86 ± 0.06	–	8.56 ± 0.14	-0.96 ± 0.04	-1.70 ± 0.07	-2.72 ± 0.10	34900
	CDT4	118	0.87 ± 0.04	0.90 ± 0.06	–	8.37 ± 0.12	-0.91 ± 0.06	-1.62 ± 0.07	-2.72 ± 0.10	35000
NGC 1637	CDT1	100	–	–	0.40	9.10	-0.88	-1.97	-3.30 ± 0.20	35000

Table 2. Physical properties of the observed H II regions.

Galaxy	Region	$L(\text{H}\alpha)$ $(10^{38} \text{ erg s}^{-1})$	$Q(\text{H})$ (10^{49} s^{-1})	ϵ	$M(\text{H II})$ $(M_\odot)$	$M^\star$ $(M_\odot)$	ϕ (arcsec)
NGC 628	H13	6.63	48.5	0.05	17900	22912	1.8
	H3	1.19	8.73	0.11	25800	2680	1.3
	H4	0.695	5.09	0.13	15000	1720	1.0
	H5	0.81	5.88	0.11	17300	1920	1.1
NGC 925	CDT1	0.91	6.67	0.41	19700	15475	1.5
	CDT4	1.27	9.27	0.25	27400	11196	2.0
NGC 1232	CDT1	20.8	152	0.008	20800	180290	1.0
	CDT2	2.27	16.6	0.07	49000	12168	0.6
	CDT3	38.5	282	0.015	25200	102900	0.9
	CDT4	48.2	353	0.02	88300	168841	1.3
NGC 1637	CDT1	1.77	13.0	–	–	10586	1.5

The Hα fluxes for regions H13, H3, and H5, uncorrected for reddening, are 669, 95 and 62×10^{-16} erg s^{-1} cm^{-2}, respectively, a factor of about 3 lower than those measured by Kennicutt & Hodge (1980) from Hα photometry (2089, 372 and 145×10^{-16} erg s^{-1} cm^{-2}). This factor reduces to about 2.4 if we take into account that their Hα filter also includes the [N II] lines which amount to about 1/3 of Hα.

Hα photographs (Hodge 1976) reveal these regions to be rather extended, and considering that our observations have been obtained through a 1.03-arcsec wide slit, this comparison implies that our derived values should be considered as lower limits. At any rate, our value for H13 agrees well with that measured by Van Zee et al. (Van Zee, private communication) which was obtained through a 2.0-arcsec diameter aperture.

For the rest of the regions we have not found any published photometric data.

The angular diameter of the emitting regions as well as the filling factors can be obtained from the ionization parameter, u, the reddening corrected Hα flux, $F(\text{H}\alpha)$ and the derived electron density, n_H, under the assumption of spherical geometry. Then

$$u = Q(\text{H})/4\pi c R^2 n_\text{H}$$

where $Q(\text{H})$ is the number of hydrogen ionizing photons s^{-1}, R is the radius of the ionized region and c is the speed of light.

The corresponding angular diameter is then found to be:

$$\phi = 0.64 \left[\frac{F(\text{H}\alpha)}{10^{-14}}\right]^{1/2} \left(\frac{u}{10^{-3}}\right)^{-1/2} \left(\frac{n_\text{H}}{10^2}\right)^{-1/2}$$

where $F(\text{H}\alpha)$ is in units of erg cm^{-2} s^{-1}, n_H is in units of cm^{-3} and ϕ is in arcsec. For the regions for which only upper limits to the electron density could be derived, a value of $n_\text{H} = 40$ cm^{-3} has been assumed. Angular diameters thus calculated do not depend on the assumed distance to the galaxy. For all the regions, we obtain angular diameters between 0.6 and 2 arcsec.

Filling factors for each observed region can also be determined from the reddening corrected Hα flux and the derived ionization parameter, according to the expression

$$\epsilon = 0.19 \left(\frac{u}{10^{-3}}\right)^{3/2} \left[\left(\frac{F(\text{H}\alpha)}{10^{-14}}\right)\left(\frac{n_\text{H}}{10^2}\right)\right]^{-1/2}$$
$$\times \left\{\left[\frac{\alpha_B(H^\circ, T)}{10^{-13}}\right]\left(\frac{D}{10}\right)\right\}^{-1}$$

where D is in Mpc and $\alpha_B(H^\circ, T)$ is the case B recombination coefficient for hydrogen for which we have used a value of 3.76×10^{-13} cm^3 s^{-1}, corresponding to $T = 7000$ K and $n_\text{H} = 100$ cm^{-3} (Osterbrock 1989). Filling factors thus derived depend inversely on the galaxy distance, D. Values between 0.008 and 0.13 are found for our adopted distances. These values are very similar to those derived for the observed H II regions in NGC 4258 (see DCTG00) and M51 (Díaz et al. 1991).

The corresponding masses of ionized hydrogen range from 1.5×10^4 M$_\odot$ for region H4 in NGC 628 to 8.8×10^4 M$_\odot$ for region CDT4 in NGC 1232.

Regions CDT1, CDT3 and CDT4 in NGC 1232 have Hα luminosities greater than 10^{39} erg s^{-1} and hence can be classified as supergiant H II regions as defined by Kennicutt (1983). The rest of the regions have Hα luminosities typical of H II regions in early spiral galaxies, although all of them are greater than 10^{37} erg s^{-1} requiring more than a single star for their ionization (Panagia 1973).

For our observed regions, all values for $Q(\text{H})$ are greater than 10^{49} photon s^{-1}. For regions CDT1, CDT3 and CDT4 in NGC 1232

values as high as 10^{51} photon s^{-1} are found. In the absence of dust and if no photons are escaping the region, a lower limit for the mass of the ionizing clusters can be estimated by means of the Hβ measured equivalent width and the Hα luminosity for each region (see Díaz 1998). Assuming a Salpeter initial mass function (IMF) with upper and lower mass limits of 100 and 0.8 M$_\odot$ respectively, the estimated ionizing cluster masses range from 1.7×10^3 M$_\odot$ for region H4 in NGC 628 to 1.80×10^5 M$_\odot$ for region CDT1 in NGC 1232. It can be inferred from these results that all the regions are ionized by relatively small clusters, except for the three supergiant H II regions in NGC 1232. Regions H3, H4 and H5 show a 10 : 1 ratio between their ionized hydrogen mass and the mass of the ionizing stellar clusters which may be then very young. Their high observed $EW(\text{H}\beta)$ values of about 200 Å support this claim.

If a given fraction of ionizing photons were absorbed by dust grains before they reach the neutral hydrogen, then the number of Lyman continuum photons emitted $Q(\text{H})_\text{em}$ by the star cluster would be higher: $Q(\text{H}) = f Q(\text{H})_\text{em}$ with $f < 1$. Therefore, our assumption of $f = 1$, i.e. absence of dust, implies that $Q(\text{H})_\text{em}$ and correspondingly M^* are lower limits. The rest of the derived nebular parameters – angular diameter, filling factor and mass of ionized hydrogen – depend on the extinction corrected Hα flux, the ionization parameter and the hydrogen density of the emitting gas. All these quantities being observable, they are not affected by the presence of absorbing dust. If f is less than unity, $Q(\text{H})_\text{em}$ would be larger than the derived $Q(\text{H})$, and, obviously, if all these emitted photons were ionizing the gas we should observe a much higher Hα flux and the nebular parameters would be different.

2.1 Wolf–Rayet populations

Relatively prominent WR features have been identified in several of the observed H II regions: H13 in NGC 628, CDT3 and, at a fainter level, CDT1 and CDT4 in NGC 1232. In all of them, the typical blue 'bump' around $\lambda 4660$ Å is observed and a red 'bump' around $\lambda 5800$ Å is also present in regions H13 (NGC 628) and CDT3 (NGC 1232). Details concerning these WR features can be found in Paper I and are summarized in Table 3.

2.1.1 Region H13 in NGC 628

Assuming a distance to NGC 628 of 7.3 Mpc (Sharina et al. 1996), and a constant extinction value through this region of $c(\text{H}\beta) = 0.29$, as derived from the Balmer and Paschen recombination lines, the total luminosities of the blue and red bumps are $(1.8 \pm 0.2) \times 10^{37}$ erg s^{-1} and $(6.5 \pm 0.6) \times 10^{36}$ erg s^{-1}, respectively. The former value comprises the features of N III $\lambda\lambda 4634$, 4640, and He II $\lambda 4686$ Å lines. The contribution of the N III lines to the blue WR bump is metallicity-dependent according to Smith (1991). In our case this contribution represents 0.45 times the total emission. Hence, the derived value for the stellar He II line luminosity is

$$L(\text{He II } \lambda 4686) = (9.5 \pm 0.4) \times 10^{36} \text{ erg s}^{-1}.$$

Based on the characteristics of the WR features, we can conclude that the observed WR stars can be classified as WN7 and using the calibration of Vacca & Conti (1992), six WN7 stars are found in region H13.

2.1.2 Region CDT3 in NGC 1232

In this case, the total luminosities of the blue and red bumps, assuming the distance to NGC 1232 of 21.5 Mpc adopted by van Zee

Table 3. WR feature intensities and equivalent widths in the observed H II regions.

Region	L(WR)/Hβ	EW(WR) (Å)	L(He II)/Hβ	EW(He II) (Å)
Region H13 (NGC 628)	0.08	8.9	0.04	4.8
Region CDT1 (NGC 1232)	0.04	2.0	0.015	0.8
Region CDT3 (NGC 1232)	0.03	5.9	0.015	2.7
Region CDT4 (NGC 1232)	0.08	10	0.03	3.9

et al. (1998) and our derived reddening constant $c(H\beta) = 0.32$, are $(4.3 \pm 1.0) \times 10^{37}$ erg s^{-1} and $(9.4 \pm 2.5) \times 10^{36}$ erg s^{-1}, respectively. The derived value for the stellar He II line luminosity is

$$L(\text{He II } \lambda 4686) = (1.95 \pm 0.50) \times 10^{37} \text{ erg s}^{-1}.$$

We classified the dominant WR stars as WN8 type. Therefore using the calibration of Vacca & Conti (1992), 12 WN8 stars are found in this region. The detection of C II, C III at $\lambda 5140$ Å could be explained by the presence of early or intermediate WC stars. It is only possible to give a lower limit to the number of WC stars because it is difficult to establish the dominant WC type (SV98). Hence, we have adopted a mean value for the average observed luminosity of WC4 stars at $\lambda 5808$ Å of 3.0×10^{36} erg s^{-1}. Therefore, at least three WC stars could be found in this region.

2.1.3 The rest of the regions in NGC 1232

Fainter WR features are found in regions CDT1 and CDT4 in NGC 1232. Region CDT1 shows a stellar He II line luminosity of $(9.5 \pm 1.0) \times 10^{36}$ erg s^{-1} compatible with the presence of six WN8 stars.

For region CDT4, the measured He II line luminosity is $(5.0 \pm 0.8) \times 10^{37}$ erg s^{-1}. Accordingly, 30 WN8 stars would be necessary to explain the observed luminosity.

3 MODELLING THE IONIZING POPULATIONS

The time-evolution of the ionizing energy output of a young star cluster can be followed with the help of stellar evolutionary tracks combined with adequate atmosphere models, and they must incorporate the most massive stars. This has been achieved in the last few years by several independent groups (e.g. Cerviño & Mas-Hesse 1994; García-Vargas, Bressan & Díaz 1995; Leitherer & Heckman 1995). In these so-called 'evolutionary synthesis models' the ionizing stellar population is represented by a cluster of coeval stars formed with a given IMF which evolve in time along to theoretical evolutionary tracks in the Hertzsprung–Russell (HR) diagram and which are able to ionize the surrounding gas. Then, the combination of the individual stellar spectral energy distributions (SED) along a given isochrone representing a given cluster age is computed. These individual SED can be taken directly from observations or from stellar atmosphere models. Although the method is rather complex and the assumption of different stellar evolution and atmosphere models can lead to different predictions for the SED of a given cluster, there are several important conclusions which are common to the work by all groups mentioned above. In particular, a hardening of the ionizing spectrum is predicted to occur between 3 and 4 Myr after the formation of the cluster as a result of the appearance of WR stars. In fact, the presence of these stars, which can be detected by the conspicuous high ionization emission lines produced in their

powerful winds (see Section 2 above) provides important clues to constrain the age of the ionizing population.

SV98 have presented very detailed models of the WR population in young star clusters, at different metallicities from $Z = 0.001$ (1/20 $Z_\odot$) to $Z = 0.04$ (2 $Z_\odot$). Their clusters are formed according to a Salpeter IMF with upper and lower mass limits of 120 and 0.8 $M_\odot$, respectively. They use the stellar evolution models by Meynet et al. (1994), which assume a mild overshooting and enhanced mass loss rate. These models have been shown to reproduce the observed WR/O star ratios in a variety of regions (Maeder & Meynet 1994). Regarding the energy output of main sequence stars they use the CoStar models (Schaerer & de Koter 1997) which include non-local thermodynamic equilibrium (non-LTE) effects, line blanketing and stellar winds, for stars with initial masses larger than 20 $M_\odot$ and Kurucz (1992) plane-parallel LTE models, including line blanketing effects, for less massive stars. The atmospheres of evolved stars in the WR phase correspond to the spherically expanding, non-LTE, unblanketed models by Schmutz, Leitherer & Gruenwald (1992).

SV98 provide accurate predictions, as a function of the cluster age, for the total number of WR stars and their subtype distribution, the broad stellar emission lines and the luminosities and equivalent widths of the two 'WR bumps' at $\lambda 4650$ and $\lambda 5808$ Å. We have used these models to derive the age of the ionizing population which contains WR stars and whose metallicity has been previously derived.

Regarding the integrated SED from the ionizing cluster, the recent models from Leitherer et al. (1999, STARBURST99) provide an almost self-consistent frame to be used in combination with the WR models described above. In fact, they use the same stellar evolution models with enhanced mass-loss rate, the same atmosphere models to describe the stars in the WR phase and cover the range of metallicities and IMF used by SV98. The only appreciable difference between both sets of models concerns the atmospheres of the main sequence stars with initial masses greater than 20 $M_\odot$ which in STARBURST99 are represented by the plane-parallel Kurucz's models implemented by Lejeune, Cuisinier & Buser (1997). We have therefore used the STARBUST99 models in order to fit the emission line spectra for our analysed regions.

3.1 Model fits to the emission line spectra

In order to predict the emission line spectrum for each analysed region, SEDs predicted by the STARBURST99 models for the stellar metallicity closest to the mean gas abundance were used as input to the latest version of CLOUDY (Ferland 1999). The models also required the gas electron density (assumed to be constant through the nebula) and elemental abundances and the ionization parameter, all of which had been previously derived (see Table 1 and Paper I for details). In all cases, we have used as input to the photoionization models the derived values of the ionization parameter, electron density and ϵ, and an inner radius adequate to reproduce the derived
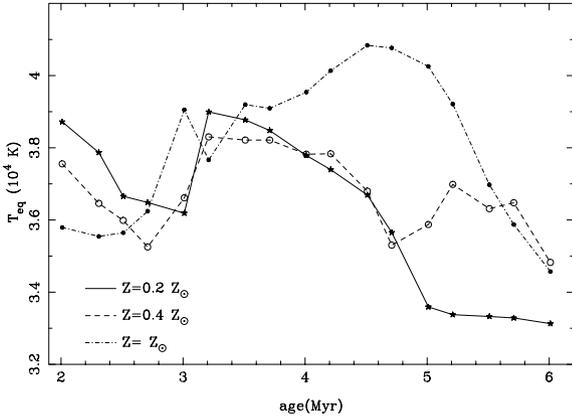
Figure 1. The equivalent temperature, defined as that of the Mihalas model atmosphere which provides the same ratio of helium to hydrogen ionizing photons, versus age for single ionizing clusters of different metallicity.

ionizing photons. In all the cases the thickness of the ionized gas shell is less than 10 per cent of the total dimensions of the region. This results in a plane-parallel geometry.

We have run models with values of the ionization parameter inside ± 0.5 dex around the derived value and cluster ages with corresponding equivalent temperatures inside ± 2000 K around the ionization temperature estimated from single star photoionization models.

The equivalent temperature for a given star cluster has been taken as the stellar effective temperature, from Mihalas (1972) model atmospheres, providing the same helium-to-hydrogen ionizing photon ratio. In all cases the nebulae are assumed to be ionization bounded. Given the run of equivalent temperature with age for ionizing clusters, which shows an important increase when the most massive stars enter the WR phase, usually more than one solution is possible. This can be seen in Fig. 1 where we show, for different metallicities of 0.2, 0.4 and 1 times solar, the cluster equivalent temperature as a function of age.

The best-fitting models are then obtained by using an optimization method that includes the more intense emission line ratios relative to Hβ. Our models do not explictly treat the physical processes associated with the presence of dust grains. However, as gas-phase measured abundances are used as input to the models, the effect of depletion onto dust grains is taken into account. The presence of dust grains will affect the thermal equilibrium of the nebula, by increasing the electron temperature and producing an enhancement of the optical forbidden lines. Nevertheless, according to Shields & Kennicutt (1995), the depletion of gas phase coolants is likely to be the most important aspect of dust in terms of its influence on the observed spectrum.

Tables 4 to 14 give, for each region, the predicted line intensities and abundances for these models together with the observed ones and their corresponding errors. As can be seen, most regions show emission line spectra which can be produced by stellar clusters of ages between 2 and 3 Myr, although in some cases other solutions are also possible.

3.2 WR populations

3.2.1 Region H13 in NGC 628

The observed WR blue and red 'bump' luminosities relative to Hβ are 0.08 and 0.03 respectively. According to the models by SV98, maximum values are found for an age of 4 Myr (0.06 and 0.03 for the blue and red 'bumps', respectively). Moreover, at the age of 4 Myr,

Table 4. Evolutionary models for region H13 in NGC 628.

Parameter	Observations	4.7 Myr
$Q(\mathrm{He})/Q(\mathrm{H})$		0.088
$Q(\mathrm{He^+})/Q(\mathrm{He})$		1.1×10^{-4}
WR/O		0.042
$\langle \log U \rangle$	-2.78 ± 0.10	-2.88
n_{e}	80	100
$12 + \log(\mathrm{O/H})$	8.24 ± 0.08	8.24
$\log(\mathrm{S/O})$	-1.83 ± 0.04	-1.78
$\log(\mathrm{N/O})$	-1.08 ± 0.04	-1.11
3727 [O II]	2960 ± 110	3852
5007 [O III]	1547 ± 10	1530
4363 [O III]	10 ± 2	10
6584 [N II]	496 ± 8	514
5755 [N II]	5 ± 1	9
6717 [S II]	204 ± 5	210
4072 [S II]	29 ± 3	30
9069 [S III]	168 ± 10	179
6312 [S III]	12 ± 1	11
$t(\mathrm{O^{2+}})$	0.98 ± 0.05	0.99
$t(\mathrm{S^{2+}})$	1.02 ± 0.03	1.02
$t(\mathrm{S^+})$	0.99 ± 0.06	0.98
$t(\mathrm{N^+})$	0.90 ± 0.06	1.04
$EW(\mathrm{H}\beta)\,(\text{Å})$	140	108
$L_{9000}\,(10^{35}\,\mathrm{erg\,s^{-1}\,Å^{-1}})$	2.9	5.7

Table 5. Evolutionary models for region H3 in NGC 628.

Parameter	Observations	2.9 Myr
$Q(\mathrm{He})/Q(\mathrm{H})$		0.13
$Q(\mathrm{He^+})/Q(\mathrm{He})$		0.00
WR/O		0.0
$\langle \log U \rangle$	-2.92 ± 0.15	-2.89
n_e	$\leqslant 40$	10
$12 + \log(\mathrm{O/H})$	8.23 ± 0.15	8.23
$\log(\mathrm{S/O})$	-1.85 ± 0.11	-1.73
$\log(\mathrm{N/O})$	-1.14 ± 0.10	-1.11
3727 [O II]	$-$	4569
5007 [O III]	1596 ± 12	1546
4363 [O III]	16 ± 2	11
6584 [N II]	470 ± 20	484
6717 [S II]	270 ± 13	234
9069 [S III]	136 ± 10	219
6312 [S III]	11 ± 1	14
$t(\mathrm{O^{2+}})$	1.17 ± 0.10	1.03
$t(\mathrm{S^{2+}})$	1.03 ± 0.05	1.06
$EW(\mathrm{H}\beta)\,(\text{Å})$	231	222
$L_{9000}\,(10^{34}\,\mathrm{erg\,s^{-1}\,Å^{-1}})$	5.6	6.2

the blue and red 'bump' equivalent widths are at their maxima, with values around 8.5 and 8 Å, respectively. These values are in excellent agreement with the observed ones: 8.9 Å for the blue bump and 6.1 Å for the red one. Regarding the individual lines, the observed values of $L(\mathrm{He\,II})/L(\mathrm{H}\beta)$ and $EW(\mathrm{He\,II})$ are 0.04 and 4.8 Å, respectively. Again, the agreement can be considered satisfactory for a single stellar population of about 4 Myr (0.02 and 3 Å, respectively, for an age of 4.1 Myr). Finally, models predict Hβ equivalent widths of 173 Å at 4 Myr and 159 Å at 4.1 Myr, to be compared with the observed value of 140 Å. Taking into account the global and individual properties of both 'bumps', the agreement between the models and the derived quantities is excellent.

Table 6. Evolutionary models for region H4 in NGC 628.

Parameter	Observations (H4)	2.5 Myr
$Q(\mathrm{He})/Q(\mathrm{H})$		0.18
$Q(\mathrm{He}^+)/Q(\mathrm{He})$		0.00
WR/O		0.0
$\langle \log U \rangle$	-2.95 ± 0.15	-2.95
n_e	$\leqslant 40$	10
$12 + \log(\mathrm{O/H})$	8.31 ± 0.15	8.18
$\log(\mathrm{S/O})$	-1.80 ± 0.11	-1.71
$\log(\mathrm{N/O})$	-0.97 ± 0.10	-1.06
3727 [O II]	–	4432
5007 [O III]	2177 ± 15	2000
6584 [N II]	527 ± 20	500
6717 [S II]	308 ± 20	245
9069 [S III]	147 ± 12	222
6312 [S III]	10 ± 2	16
$t(\mathrm{O}^{2+})$	0.94	1.09
$t(\mathrm{S}^{2+})$	0.95 ± 0.05	1.11
$EW(\mathrm{H}\beta)\,(\text{Å})$	220	290
$L_{9000}\,(10^{34}\,\mathrm{erg\,s^{-1}\,\text{Å}^{-1}})$	2.9	4.2

Table 7. Evolutionary models for region H5 in NGC 628.

Parameter	Observations (H5)	2.95 Myr
$Q(\mathrm{He})/Q(\mathrm{H})$		0.13
$Q(\mathrm{He}^+)/Q(\mathrm{He})$		0.00
WR/O		0.0
$\langle \log U \rangle$	-2.97 ± 0.15	-3.20
n_e	$\leqslant 40$	10
$12 + \log(\mathrm{O/H})$	8.34 ± 0.15	8.36
$\log(\mathrm{S/O})$	-1.67 ± 0.10	-1.71
$\log(\mathrm{N/O})$	-1.07 ± 0.10	-1.16
3727 [O II]	–	5461
5007 [O III]	529 ± 8	692
6584 [N II]	631 ± 43	750
6717 [S II]	391 ± 24	400
9069 [S III]	149 ± 10	213
6312 [S III]	7 ± 2	11
$t(\mathrm{O}^{2+})$	0.79	0.97
$t(\mathrm{S}^{2+})$	0.82 ± 0.06	1.0
$EW(\mathrm{H}\beta)\,(\text{Å})$	205	222
$L_{9000}\,(10^{34}\,\mathrm{erg\,s^{-1}\,\text{Å}^{-1}})$	3.4	4.2

Table 8. Evolutionary models for region CDT1 in NGC 1232.

Parameter	Observations	2.3 Myr	5.7 Myr
$Q(\mathrm{He})/Q(\mathrm{H})$		0.10	0.098
$Q(\mathrm{He}^+)/Q(\mathrm{He})$		3.5×10^{-5}	1.8×10^{-4}
WR/O		0.03	>0.48
$\langle \log U \rangle$	-2.95 ± 0.20	-2.95	-3.10
n_e	130	130	130
$12 + \log(\mathrm{O/H})$	8.95 ± 0.20	9.05	9.05
$\log(\mathrm{S/O})$	-1.81 ± 0.10	-1.81	-1.81
$\log(\mathrm{N/O})$	-0.81 ± 0.08	-0.81	-0.81
3727 [O II]	1490 ± 70	2190	1422
5007 [O III]	229 ± 4	263	239
5755 [N II]	4 ± 1	7	5
6584 [N II]	1040 ± 21	1600	1288
6717 [S II]	357 ± 8	340	387
6312 [S III]	2 ± 1	4	2
9069 [S III]	197 ± 13	291	170
$t(\mathrm{N}^+)$	0.67 ± 0.06	0.63	0.58
$t(\mathrm{O}^{2+})$	0.45	0.56	0.49
$t(\mathrm{S}^{2+})$	0.54 ± 0.05	0.60	0.53
$EW(\mathrm{H}\beta)\,(\text{Å})$	48	328	31
$L_{9000}\,(10^{36}\,\mathrm{erg\,s^{-1}\,\text{Å}^{-1}})$	4.2	0.9	4.7

Table 9. Evolutionary models for region CDT2 in NGC 1232.

Parameter	Observations	3.0 Myr	4.5 Myr
$Q(\mathrm{He})/Q(\mathrm{H})$		0.155	0.130
$Q(\mathrm{He}^+)/Q(\mathrm{He})$		5.4×10^{-4}	0.062
WR/O		0.01	0.1
$\langle \log U \rangle$	-2.95 ± 0.15	-3.05	-3.10
n_e	$\leqslant 40$	10	10
$12 + \log(\mathrm{O/H})$	8.61 ± 0.15	8.60	8.55
$\log(\mathrm{S/O})$	-1.81	-1.71	-1.71
$\log(\mathrm{N/O})$	-1.15	-1.15	-1.15
3727 [O II]	4180 ± 220	4313	4026
5007 [O III]	1350 ± 20	1375	1334
6584 [N II]	717 ± 30	710	694
6717 [S II]	537 ± 15	517	523
9069 [S III]	191 ± 15	294	257
$t(\mathrm{O}^{2+})$	–	0.79	0.81
$t(\mathrm{S}^{2+})$	–	0.83	0.84
$EW(\mathrm{H}\beta)\,(\text{Å})$	84	267	111
$L_{9000}\,(10^{36}\,\mathrm{erg\,s^{-1}\,\text{Å}^{-1}})$	1.4	0.12	0.2

Therefore we can assign an age of 4–4.1 Myr to the ionizing stellar population that would be responsible for the WR emission features.

3.2.2 *H II regions in NGC 1232*

From the four H II regions of NGC 1232 analysed in Paper I, three of them present weak blue WR 'bumps' (CDT1, CDT3 and CDT4). Special attention must be paid to region CDT1 showing a metallicity close to solar. For this region the observed WR blue 'bump' luminosity relative to Hβ is 0.04, extremely low for a high metallicity H II region. A very low value is also found for the blue 'bump' equivalent width, near 2 Å. Regarding the stellar He II luminosity and equivalent width, values of 0.015 and 0.8 Å are found. According to models by SV98, these low values could be produced by an evolved ionizing population with an age around 7 Myr. This population would provide a blue 'bump' equivalent width of 2.4 Å,

consistent with the observed value, but would overestimate its luminosity relative to Hβ by more than an order of magnitude (0.55 versus 0.04), while providing an Hβ equivalent width of only 4 Å versus the observed one of 48 Å.

Low values of blue 'bump' luminosities and equivalent widths are also found for early ages, at the beginning of the WR phase. A cluster of 2.3 Myr of age provides values of the blue 'bump' luminosity 0.02 with respect to Hβ and 5.17 Å for its equivalent width, roughly consistent with the observations. This population, however, would produce an equivalent width of Hβ of 312 Å, much higher than observed.

Similarly low ages are found when this sort of analysis is applied to regions CDT3 and CDT4. Region CDT3 shows a WR 'bump' luminosity relative to Hβ of 0.03. Taking into account its derived metallicity ($12 + \log \mathrm{O/H} = 8.56$ or $Z = 0.008$), SV98 predicts this

Table 10. Evolutionary models for region CDT3 in NGC 1232.

Parameter	Observations	2.8 Myr	4.8 Myr
$Q(\mathrm{He})/Q(\mathrm{H})$		0.088	0.082
$Q(\mathrm{He}^+)/Q(\mathrm{He})$		5.1×10^{-6}	0.25
WR/O		0.0	0.027
$\langle \log U \rangle$	-2.72 ± 0.10	-2.80	-2.82
n_e	223	230	230
$12 + \log(\mathrm{O/H})$	8.56 ± 0.14	8.58	8.55
$\log(\mathrm{S/O})$	-1.70 ± 0.07	-1.70	-1.71
$\log(\mathrm{N/O})$	-0.96 ± 0.04	-1.00	-0.96
3727 [O II]	3180 ± 150	4471	2868
5007 [O III]	842 ± 13	823	1972
6584 [N II]	892 ± 30	894	890
5755 [N II]	8 ± 2	10	9
6717 [S II]	333 ± 10	301	329
4072 [S II]	48 ± 6	40	43
9069 [S III]	229 ± 10	340	271
6312 [S III]	8 ± 2	13	10
$t(\mathrm{O}^{2+})$	0.69	0.82	0.81
$t(\mathrm{S}^{2+})$	0.74 ± 0.05	0.85	0.84
$t(\mathrm{S}^+)$	0.90 ± 0.06	0.88	0.84
$t(\mathrm{N}^+)$	0.86 ± 0.06	0.89	0.87
$EW(\mathrm{H}\beta)\,(\text{Å})$	189	257	60
$L_{9000}\,(10^{36}\,\mathrm{erg\,s^{-1}\,Å^{-1}})$	1.6	1.9	4.9

Table 11. Evolutionary models for region CDT4 in NGC 1232.

Parameter	Observations	2.8 Myr	4.8 Myr
$Q(\mathrm{He})/Q(\mathrm{H})$		0.088	0.082
$Q(\mathrm{He}^+)/Q(\mathrm{He})$		5.1×10^{-6}	0.25
WR/O		0.0	0.027
$\langle \log U \rangle$	-2.72 ± 0.10	-2.65	-2.73
n_e	118	100	100
$12 + \log(\mathrm{O/H})$	8.37 ± 0.12	8.45	8.45
$\log(\mathrm{S/O})$	-1.62 ± 0.07	-1.60	-1.65
$\log(\mathrm{N/O})$	-0.91 ± 0.06	-0.95	-0.95
3727 [O II]	2530 ± 120	3982	2582
5007 [O III]	1162 ± 8	1093	2193
6584 [N II]	758 ± 40	729	730
5755 [N II]	8 ± 1	10	9
6717 [S II]	307 ± 20	257	305
9069 [S III]	249 ± 10	373	283
6312 [S III]	13 ± 2	16	12
$t(\mathrm{O}^{2+})$	0.84	0.86	0.85
$t(\mathrm{S}^{2+})$	0.87 ± 0.04	0.90	0.87
$t(\mathrm{N}^+)$	0.90 ± 0.06	0.94	0.91
$EW(\mathrm{H}\beta)\,(\text{Å})$	138	256	60
$L_{9000}\,(10^{36}\,\mathrm{erg\,s^{-1}\,Å^{-1}})$	7.1	2.4	6.2

Table 12. Evolutionary models for region CDT1 in NGC 1637.

Parameter	Observations	2.8 Myr	5.9 Myr
$Q(\mathrm{He})/Q(\mathrm{H})$		0.082	0.064
$Q(\mathrm{He}^+)/Q(\mathrm{He})$		1.26×10^{-4}	1.20×10^{-4}
WR/O		0.24	>0.9
$\langle \log U \rangle$	-3.30 ± 0.20	-3.25	-3.15
n_e	100	100	100
$12 + \log(\mathrm{O/H})$	9.10	9.20	9.10
$\log(\mathrm{S/O})$	-1.97	-1.90	-1.80
$\log(\mathrm{N/O})$	-0.88	-0.87	-0.87
3727 [O II]	1170 ± 60	1116	1031
5007 [O III]	84 ± 10	90	90
6584 [N II]	1037 ± 60	1212	1039
6717 [S II]	335 ± 20	359	379
9069 [S III]	99 ± 9	131	141
t_{adopt}	0.40	0.46	0.46
$EW(\mathrm{H}\beta)\,(\text{Å})$	74	137	22
$L_{9000}\,(10^{35}\,\mathrm{erg\,s^{-1}\,Å^{-1}})$	2.6	1.1	5.5

Table 13. Evolutionary models for region CDT1 in NGC 925.

Parameter	Observations	5.8 Myr	5.9 Myr
$Q(\mathrm{He})/Q(\mathrm{H})$		0.124	0.076
$Q(\mathrm{He}^+)/Q(\mathrm{He})$		7.58×10^{-4}	2.86×10^{-3}
WR/O		0.023	0.022
$\langle \log U \rangle$	-3.00 ± 0.30	-3.15	-2.95
n_e	$\leqslant 40$	10	10
$12 + \log(\mathrm{O/H})$	8.52 ± 0.20	8.62	8.52
$\log(\mathrm{S/O})$	-1.83	-1.71	-1.71
$\log(\mathrm{N/O})$	-1.07	-1.17	-1.17
3727 [O II]	2880 ± 110	3580	3428
5007 [O III]	849 ± 14	1041	809
6584 [N II]	568 ± 28	673	577
6717 [S II]	577 ± 30	601	390
9069 [S III]	125 ± 9	233	229
t_{adopt}	0.86	0.74	0.78
$EW(\mathrm{H}\beta)\,(\text{Å})$	22	25	23
$L_{9000}\,(10^{35}\,\mathrm{erg\,s^{-1}\,Å^{-1}})$	9.8	2.97	3.3

value for a cluster with an equivalent width of Hβ of $\sim$200 Å, which is in excellent agreement with our measured value of 189 Å. This corresponds to an instantaneous burst with age between 3.1 and 3.5 Myr. Furthermore, the predicted blue 'bump' equivalent width at this age ranges from 5.5 to 10 Å in good agreement with the observed one (5.9 Å). Consistency is also found for the weak red 'bump', whose observed values for both the luminosity and equivalent width are 0.007 and 2.0 Å respectively that should be compared with the predicted ones (0.006–0.015 and 2.2–4.2 Å, respectively). Regarding the He II line luminosity and equivalent width, our observed values are 0.015 and 2.7 Å in excellent agreement, again, with the predicted ones (0.011–0.007 and 2.15–0.75 Å respectively).

In the case of region CDT4, the WR blue 'bump' luminosity relative to Hβ is 0.08. For its derived metallicity ($12 + \log \mathrm{O/H} = 8.37$ or $Z = 0.006$). A value of 0.11 is predicted for an instantaneous burst of 4.1 Myr at $Z = 0.008$, which in turn predicts an Hβ equivalent width of 105 Å. This value is consistent with the observed one of 138 Å. The observed WR blue 'bump' equivalent width is 10 Å in good agreement with the predicted value of 10.8 Å at this age. The He II line intensity and equivalent width are again fully consistent with the corresponding predicted values (0.03 versus 0.04 and 3.9 Å versus 3.7 Å, respectively).

Therefore, relatively young single ionizing populations between 3 and 4 Myr are required to reproduce the observed WR features in regions CDT3 and CDT4. For region CDT1, no consistent solution is found. An old cluster of 7 Myr would roughly fit the equivalent width of the WR blue 'bump' but would overpredict its luminosity with respect to Hβ by more than an order of magnitude and underpredict the Hβ equivalent width by about the same amount. On the other hand, young clusters of about 2.5 Myr predict WR blue 'bump' luminosities and equivalent widths in agreement with observations but Hβ equivalent widths larger than observed by almost a factor of 10.

Table 14. Evolutionary models for region CDT4 in NGC 925.

Parameter	Observations	2.8 Myr	5.9 Myr	Composite
$Q(\text{He})/Q(\text{H})$		0.088	0.076	0.083
$Q(\text{He}^+)/Q(\text{He})$		5.13×10^{-6}	2.86×10^{-3}	1.13×10^{-3}
WR/O		0.00	0.022	
$\langle \log U \rangle$	-3.00 ± 0.25	-3.20	-3.32	-2.97
n_e	$\leqslant 40$	10	10	10
$12 + \log(\text{O/H})$	8.41 ± 0.20	8.47	8.47	8.47
$\log(\text{S/O})$	-1.83	-1.71	-1.71	-1.71
$\log(\text{N/O})$	-1.01	-1.17	-1.17	-1.17
3727 [O II]	2820 ± 120	5133	4164	4242
5007 [O III]	737 ± 10	257	328	725
6584 [N II]	593 ± 18	764	724	609
6717 [S II]	437 ± 15	508	593	372
9069 [S III]	160 ± 10	233	174	248
t_{adopt}	0.93	0.87	0.83	0.84
$EW(\text{H}\beta)\,(\text{Å})$	47	255	23	48
$L_{9000}\,(10^{35}\ \text{erg s}^{-1}\ \text{Å}^{-1})$	4.4	0.36	1.95	2.3
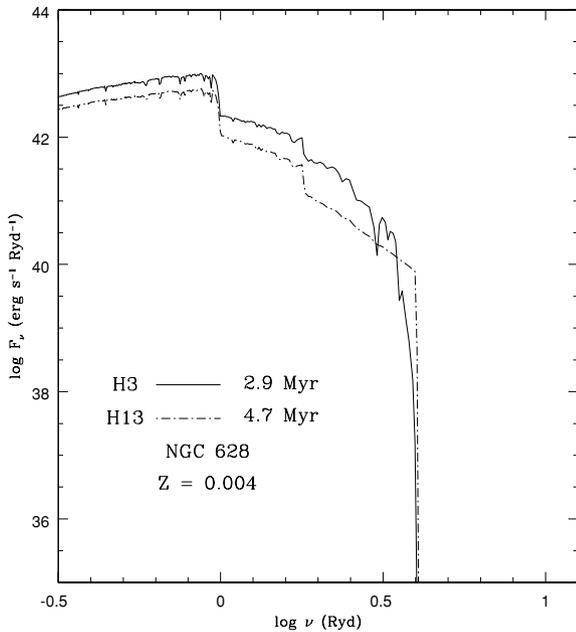
Figure 2. Spectral energy distributions of the ionizing clusters able to reproduce the emission line spectra of regions H13 and H3 in NGC 628.

4 DISCUSSION

The analysis of emission line spectra of a giant extragalactic H II region (GEHR) containing WR stars offers an unique opportunity to test our present ideas about the evolution of star-forming regions and check on the accuracy of current stellar evolution and atmosphere models. Most works on stellar population synthesis of ionized regions assume that the ionizing population responsible for the observed gas emission belongs to a single star cluster created in a unique star formation episode. Therefore the WR emission features can be used to date these star clusters which, in turn, should reproduce the observed emission line intensities if the other parameters controlling the emission line spectra, namely elemental abundances, particle density and ionization parameter, are known. Four of our observed H II regions meet all these requirements.

4.1 H II regions with observed WR features

4.1.1 H13 in NGC 628

H13 in NGC 628 has a mean oxygen abundance of $12 + \log(\text{O/H}) = 8.24$, about 0.2 times solar if $12 + \log(\text{O/H}) = 8.92$ is assumed as the solar value. The models of SV98 for this metallicity reproduce the observed WR features for an ionizing cluster of 4.1 Myr which produces an $\text{H}\beta$ equivalent width of 159 Å. In this cluster the proportion of WR to O stars is WR/O $= 5.1 \times 10^{-2}$. As both SV98 and STARBURST99 models make use of the same stellar evolution prescriptions (see Section 3), we have assumed that a STARBURST99 model of a cluster of metallicity 0.2 times solar which contains the same WR/O star ratio provides the spectral energy distribution of the ionizing radiation. This model, however, provides an [O III]λ5007 Å line emission which is higher than observed by a factor of about 4. Also, the [S II] and [N II] lines are down by a factor of about 2 and the equivalent width of $\text{H}\beta$ is somewhat larger than observed.

On the other hand, our best photoionization model corresponds to an age of 4.7 Myr producing an $\text{H}\beta$ equivalent width of 108 Å. The most appreciably discrepancy between predicted and observed emission line ratios is found for the [O II]λ3727 Å line which is overestimated in the model by a factor of 30 per cent. This line is the one more affected by reddening as the rest of the emission lines are measured relative to a nearby hydrogen recombination line. The rest of the spectrum is reproduced remarkably well (see Table 4), including the equivalent width of $\text{H}\beta$ (inside 30 per cent) and the continuum luminosity at 9000 Å (inside a factor of 2). Clusters younger than 4.7 Myr have a spectral energy distribution which results too hard to explain the observations. According to SV98 models a cluster of this age would produce WR luminosities and equivalent widths which are lower than observed by a factor of two, corresponding to a WR/O ratio of 4.2×10^{-2}. Given the uncertainties involved in the different models employed, we can conclude that a single star cluster with age between 4.0 and 4.7 Myr fit all the observations adequately. The ionizing spectrum of the cluster of 4.7 Myr is shown in Fig. 2.

4.1.2 CDT1 in NGC 1232

Region CDT1 in NGC 1232 shows the highest oxygen abundance of the regions with WR features [$12 + \log(\text{O/H}) = 8.95$, about
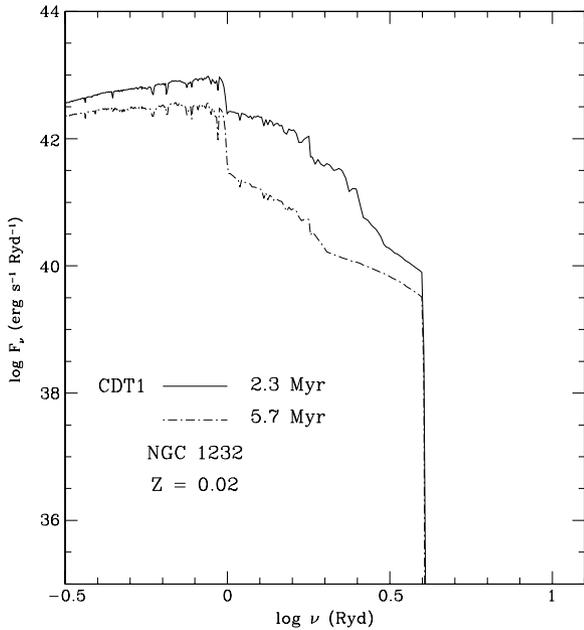
Figure 3. Spectral energy distributions of the ionizing clusters able to reproduce the emission line spectrum of region CDT1 in NGC 1232.

Table 15. Ionizing populations for region CDT1 in NGC 1232.

Parameter	2.4 Myr	7.1 Myr	Composite
Q(H) (10^{50} s^{-1})	13.8	1.38	15.2
Q(He) (10^{48} s^{-1})	140	0.17	140
L(Hβ) (10^{37} erg s^{-1})	66.1	6.61	72.7
M* (10^4 M$_\odot$)	2.73	15.3	18.0
L(WR)/Hβ	0.029	0.0	0.026
EW(WR) (Å)	7.3	0.0	1.1
EW(Hβ) (Å)	312	5.4	51
L(9000) (10^{36} erg s^{-1} Å^{-1})	0.88	4.75	5.63
$\langle \log U \rangle$	-2.88	-3.88	-2.85
3727 [O II]	2119	551	1904
4861 Hβ	1000	1000	1000
5007 [O III]	294	0	260
6584 [N II]	1489	944	1384
6717 [S II]	304	474	281
9069 [S III]	295	15	277

4.1.3   CDT3 in NGC 1232

For region CDT3 in NGC 1232, the SV98 model which best reproduces the observed WR features has an age of 3.1 Myr. The ratio of WR to O stars is WR/O $= 5.4 \times 10^{-2}$. A STARBURST99 model cluster with the same WR/O ratio has 3.3 Myr of age and provides an Hβ equivalent with of 159 Å, close to the observed one (189 Å). However, when used as input to the photoionization model, this cluster provides [O III]λ5007 Å line emission higher than observed by a factor of about 5. This is not unexpected, as the equivalent temperature corresponding to this cluster is around 38 200 K, while that estimated from photoionization models is only 34 900 K (see Paper I). Clusters slightly older, also reproducing the observed WR features within the errors, have larger WR/O number star ratios (up to 8.3×10^{-2}) and therefore their spectral energy distributions result even harder.

From the analysis of the emission line spectrum, two ionizing clusters are found with the same Q(He)/Q(H) number photon ratio corresponding to the derived equivalent temperature of 34 900 K (see Table 10 and Fig. 4). The younger of these clusters, however, do not contain WR stars (WR/O = 0.0) and the oldest has WR/O $= 2.65 \times 10^{-2}$, a factor of about 2 lower than required to reproduce the WR features.

From the point of view of ionization, the combination of two clusters with ages 2.8 and 4.8 Myr contributing approximately 90 per cent and 10 per cent to the total number of ionizing photons would reproduce the emission line spectrum rather well, except for the [O II]3727 Å line which results about 40 per cent higher in the model. Also, the equivalent width of Hβ and the continuum light at λ9000 Å are well reproduced. However, for this population, the luminosity and equivalent width of the WR blue 'bump' are lower than observed by factors of about 15 and 25, respectively.

4.1.4   CDT4 in NGC 1232

A similar situation is found for region CDT4. The SV98 model which best reproduces the observed WR features has an age of 4.1 Myr. The ratio of WR to O stars is WR/O $= 9.2 \times 10^{-2}$, the highest of all the observed regions. The STARBURST99 model cluster of the same age also has the same WR/O ratio and provides an Hβ equivalent width of 131 Å, that should be compared with the observed one of 138 Å. When introduced as input in the photoionization code, this cluster reproduces the emission line spectrum
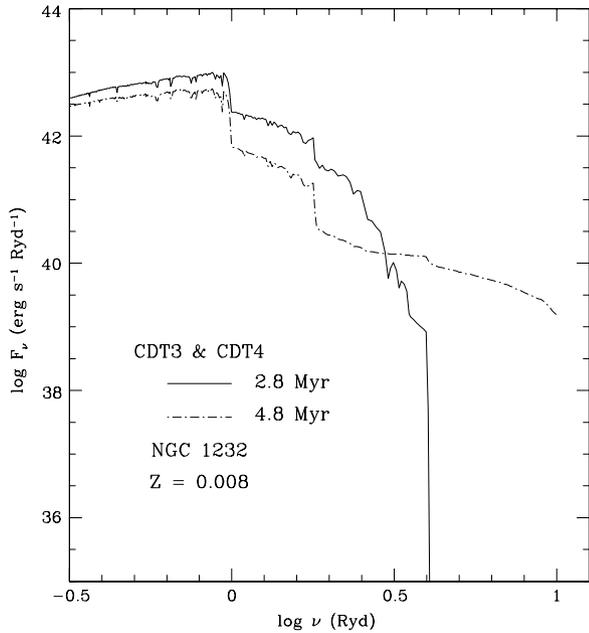
solar if $12 + \log$(O/H)$_\odot = 8.92$]. As explained above, no consistent solution for a single ionizing population is found to reproduce the observed WR features. For this region, two star clusters, with 2.3 and 5.7 Myr respectively, provide Q(He)/Q(H) ratios nearly identical and corresponding to the stellar effective temperature of about 35 000 K, in the Mihalas scale, which reproduces the general features of the emission line spectrum (see Paper I). Their ionizing spectra are shown in Fig. 3.

The oldest of the two clusters yields emission line ratios in better agreement with the observations and an equivalent width of Hβ closer to the observed one (see Table 8). Clusters older than this cannot provide the necessary photons to ionize the region. SV98 models for this age (5.7 Myr), however, give WR features with luminosities relative to Hβ which are a factor of about 10 larger than observed. On the other hand, the young 2.3-Myr cluster is more successful in reproducing both the WR blue 'bump' luminosity and the equivalent width, although it overpredicts the equivalent width of Hβ. These two facts taken together point to the presence of a composite population with, at least two clusters: a young one of about 2.5 Myr containing the WR stars and an older one providing the bulk of the continuum light at λ4800 Å. We have therefore run a model using as ionizing source the combination of the spectral energy distributions of two ionizing clusters of 2.4 and 7.1 Myr of age calculated with the STARBURST99 code in which the youngest of the two provides 10 times the number of ionizing photons emitted by the oldest. This cluster contains the same WR/O star ratio as the SV98 model reproducing the observed WR features. The computed photoionization model is able to reproduce, with a reasonable degree of accuracy, most of the observational constraints: the emission line spectrum, the WR features both in luminosity and equivalent width, the equivalent width of Hβ and the continuum luminosity at 9000 Å. The characteristics of the two clusters, together with the corresponding predictions of the photo-ionization model are given in Table 15. The particle density and the elemental abundances have been kept at their derived values given in Table 1.

Figure 4. Spectral energy distributions of the ionizing clusters able to reproduce the emission line spectra of regions CDT3 and CDT4 in NGC 1232.

Figure 5. Spectral energy distributions of the ionizing clusters able to reproduce the emission line spectra of regions H4 and H5 in NGC 628.

satisfactorily, except for the [O III]λ5007 Å line which is higher than observed by a factor of about 3. Again this is related to the hardness of the ionizing continuum which provides a Q(He)/Q(H) ratio of 0.18 which corresponds to an equivalent temperature of 37 800 K, while the corresponding one derived from the emission line spectrum is only 35 000 K (see Paper I).

Again, the analysis of the emission line spectrum indicates two possible star clusters as ionizing sources whose ages coincide with those found for region CDT3 (see Table 11 and Fig. 4). Therefore, regarding the ionization, the same discussion above applies to this region: it is possible to find a combination of ionizing clusters which reproduces the emission line spectrum well, but predicts WR feature luminosities and equivalent widths well below the observed values.

4.2 H II regions with no WR features observed

In the rest of the regions, no WR features are observed and therefore the estimation of the age of the ionizing populations must be made with the only help of the analysis of the emission line spectra. Out of the two solutions found for region H3 in NGC 628, the cluster with 4.5 Myr provides the best fit to the emission line spectrum (Table 5). Most line ratios are predicted to better than 10 per cent. The predicted Hβ equivalent width however, is 60 per cent lower than observed. On the other hand, this cluster has a WR/O number star ratio of 5.8×10^{-2}, which would provide a WR blue 'bump' luminosity relative to Hβ of 0.036 and an equivalent width of 3.78 Å, that should be observable. The younger cluster, of 2.9 Myr, does not have WR stars and, although the fit to the emission line spectrum is slightly worse, it does predict adequately both the equivalent width of Hβ and the continuum luminosity at λ9000 Å. Therefore, a single young ionizing cluster of less than 3 Myr, in an evolutionary state prior to the appearance of WR stars, produces a satisfactory fit to all the observational constraints. The spectral energy distribution of the 2.9 Myr cluster is shown in Fig. 2.

The ionization of regions H4 and H5 also requires young clusters without WR stars. Clusters of 2.5 Myr and 2.9 Myr respectively
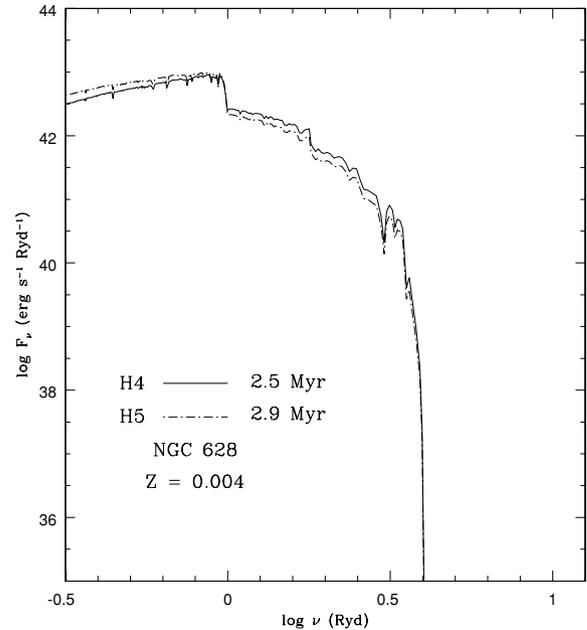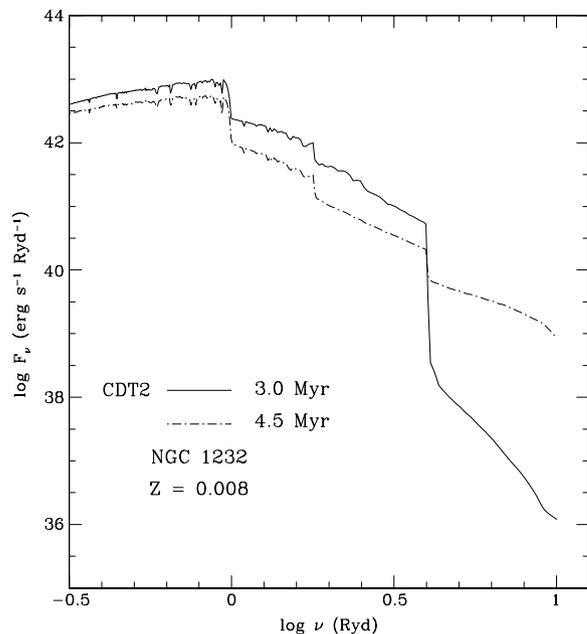

Figure 6. Spectral energy distributions of the ionizing clusters able to reproduce the emission line spectrum of region CDT2 in NGC 1232.

reproduce satisfactorily the emission line spectra, the Hβ equivalent widths and the luminosity at 9000 Å (see Tables 6 and 7). The cluster in H5 seems to be slightly older than that in H4 and the ionization parameter in this region is lower by a factor of about 2. The SEDs of the two ionizing clusters is shown in Fig. 5.

The region in NGC 1232 not showing WR features, CDT2, also allows for two possible ionizing clusters (see Table 9 and Fig. 6). According to the STARBURST99 models, the oldest one, with 4.5 Myr, has a WR/O star ratio of 0.1 which, in SV98 models, gives a WR blue 'bump' luminosity and an equivalent width of 0.1 and 6.8 Å, respectively. On the other hand, the youngest cluster with 3 Myr,
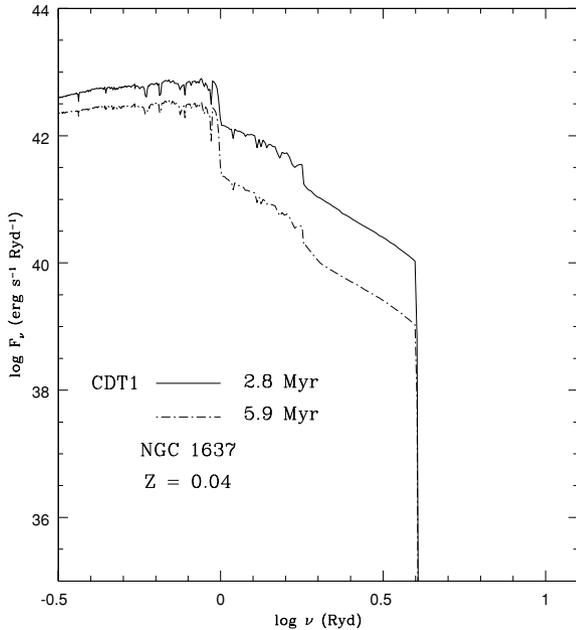
Figure 7. Spectral energy distributions of the ionizing clusters able to reproduce the emission line spectrum of region CDT1 in NGC 1637.
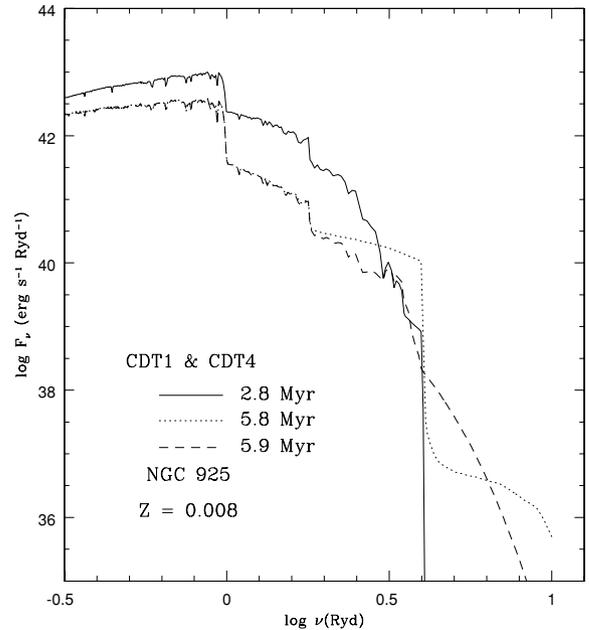

Figure 8. Spectral energy distributions of the ionizing clusters able to reproduce the emission line spectra of regions CDT1 and CDT4 in NGC 925.

has a WR/O star ratio of only 0.01 and provides WR blue 'bump' luminosity relative to Hβ and equivalent width of 0.01 and 2.34 Å respectively. Based on the fact that no WR features are observed, we consider this latter cluster as a better candidate for the ionization of the region. Nevertheless, it does not seem to be the only population present since the low observed value of the Hβ equivalent width points to an underlying population that would contribute 70 per cent to the luminosity at Hβ. The WR blue 'bump' equivalent width would be consequently lowered to only 0.7 Å which is consistent with the lack of detection of the feature.

The other region of the sample showing a high metallicity (about twice solar) is CDT1 in NGC 1637. Two ionizing clusters with $Z = 0.04$ are able to reproduce the observed emission line spectrum to the same degree of accuracy and they produce Hβ equivalent widths higher and lower than observed, respectively (see Table 12 and Fig. 7). Also, the observed λ9000 Å luminosity is intermediate to that predicted by the two clusters. Therefore, the best solution would seem to consist of a combination of the two. We should, however, keep in mind that, according to models, both clusters contain WR stars with WR/O ratios between 0.14 and 14. The oldest cluster would provide large values of both the blue 'bump' luminosity and the equivalent width (0.7 and 13 Å) while the younger one would provide about the same equivalent width but a luminosity lower by a factor of about 5 (0.14). Therefore, based on the fact that no WR features are observed, we feel that the most plausible solution would be the combination of a young ionizing cluster providing the bulk of the ionization and an underlying population which would lower the equivalent width of Hβ to the observed values. This underlying population should contribute 50 per cent of the continuum luminosity at λ4861 Å.

Finally, not much can be said about the two regions in NGC 925 (see Fig. 8). Both of them show a metallicity of about $12 + \log(O/H) \simeq 8.5$, although, due to the non detection of suitable temperature sensitive lines, the uncertainty in the derived oxygen abundance is high (± 0.20). In the case of CDT1, the emission line spectrum can be adequately reproduced by relatively old

ionizing clusters of slightly different age and metallicity (5.8 Myr and $12 + \log(O/H) = 8.52$ or 5.9 Myr and $12 + \log(O/H) = 8.62$) with the best solution probably being in between (see Table 13). There is however some room for contribution by a non ionizing cluster since the luminosity at λ9000 Å is predicted to be lower than observed by a factor of about 3.

In the case of CDT4, the 5.9-Myr cluster predicts an equivalent width of Hβ lower than observed by a factor of about 2, whereas a young cluster without WR stars (2.8 Myr) gives a value much larger than observed (Table 14). It is, however, possible to find a satisfactory solution by considering the combination of two clusters of 2.8 and 5.9 Myr with this former one, providing 60 per cent of the total number of ionizing photons. This solution is also listed in Table 14.

4.3 Global analysis

In summary, out of the 11 analysed regions, only the four in NGC 628 seem to be consistent with the presence of single ionizing star clusters; all of them show relatively low abundances. For the rest of the regions, at least two populations are needed: a young one, with age between 2.5 and 3 Myr, which provides most of (or all) the ionizing photons, and an older one which contributes a substantial fraction of the continuum luminosity. This second population also contains an important fraction of the mass of the composite cluster. The difference in age between the two populations is not very large, 3–10 Myr.

Composite populations for H II regions have been found in previous work by Mayya & Prabhu (1996) and by Díaz et al. (2000b) for disc and circumnuclear objects, respectively, from broad-band and Hα photometry. A spectrophotometric analysis of circumnuclear H II regions in NGC 3310 (Pastoriza et al. 1993) and NGC 7714 (García-Vargas et al. 1997) also reveals the presence of composite populations and even in the young H II region 30 Dor in the LMC a spread in age for the stellar populations has been found (Selman et al. 1999).

This scenario is able to reproduce both the emission line spectrum and the WR features of the high metallicity region CDT1 in NGC 1232. It is nevertheless not sufficient to explain the observations in the two intermediate metallicity H II regions in NGC 1232 with WR features: CDT3 and CDT4. For these two regions, no consistent solution can be found. While the models by SV98 consistently provide excellent fittings to the observed WR properties, the evolutionary models by STARBURST99 result too hard to explain the observed emission line spectra.

Several solutions can be suggested such as the inadequacy of the stellar evolutionary tracks, uncertainties in the computation of stellar atmosphere models or the everlasting question of temperature fluctuations within these regions that would underestimate the true abundances.

The fact that the WR features are adequately reproduced by SV98 models seem to imply that the evolutionary tracks are able to predict the right relative numbers of WR/O stars, and their different subtypes at the derived abundances. These relative numbers, combined with the observed emission line luminosities of the individual WR stars, and the predicted continuum energy distribution of the ionizing population, predict emission line intensities and equivalent widths of the WR stars that are in excellent agreement with observations. This can be seen in Fig 9. The upper and lower panels respectively show the predicted emission line intensities and equivalent widths of the WR blue 'bump' for different metallicities: 0.2 solar, 0.4 solar and solar together with the data corresponding to the four observed objects. Solid symbols correspond to the observed data. In the case of CDT1 in NGC 1232, for which a composite population is found, two open symbols are shown, one corresponding to the predictions for a single ionizing cluster, and another one including the contribution to the Hβ and continuum luminosity of the cluster not containing WR stars. For regions CDT3 and CDT4 observations and predictions are nearly identical for the respective clusters and therefore only one symbol is shown. As we can see, the agreement for the three regions in NGC 1232 is surprisingly good. For region H13 in NGC 628 the predicted and observed values (solid and open symbols) agree inside a factor of about 2. We therefore conclude that, regarding the WR star populations, the currently assumed stel-

lar evolution, including a high mass-loss, is adequate to match the observations, at least for intermediate and high metallicities. The worse agreement found for region H13 in NGC 628, whose WR feature luminosity and equivalent width seem to indicate a slightly higher metallicity, might in principle be attributed to the presence of temperature fluctuations, which do not need to be invoked in the other cases.

The third possible source of disagreement concerns the existing uncertainties in modelling the atmospheres of high mass stars of O and WR types. Our results seem to point to an overestimation of the hardness of the spectral energy distribution of the stars in the WR phase, which is more apparent for intermediate to high metallicities. The same sort of effect has been found by DCTG00 for region 74C in NGC 4258 and Esteban et al. (1993) for the galactic WR nebula M1–67. These latter authors, from stellar and nebular spectroscopic analyses, concluded that lower temperatures were required from the photoionization models for late-type WN (WNL) stars. In their study they used the unblanketed WR models of Schmutz et al. (1992). A subsequent reanalysis of this region has been made by Crowther et al. (1999) using blanketed model atmospheres. In this case the resulting ionizing spectrum is much softer and reproduces better the observations although some important discrepancies, like a negligible He I λ5876 Å line intensity, which is none the less observed, and the overprediction of [O II] λ3727 Å and [N II] λ6584 Å by factors of 3 and 2 respectively, still remain.

It should, however, be recalled that all results discussed above are based on ionization bounded models. An interpretation of the emission line spectra of H II region with WR features on the basis of matter bounded models has been presented in Castellanos, Díaz & Tenorio-Tagle (2002). Models of this kind have been found to provide excellent fittings to the observations of H13 in NGC 628, CDT3 in NGC 1232 and 74C in NGC 4258 using both SV98 and STARBURST99 models. These models would point to an important leakage of ionizing photons depending on both the metallicity and evolutionary state of the region.

Certainly, the inclusion of line blanketing in the model atmospheres of WR stars, which is already included in the CoStar (Schaerer & de Koter 1997) and Lejeune et al. (1997) models is
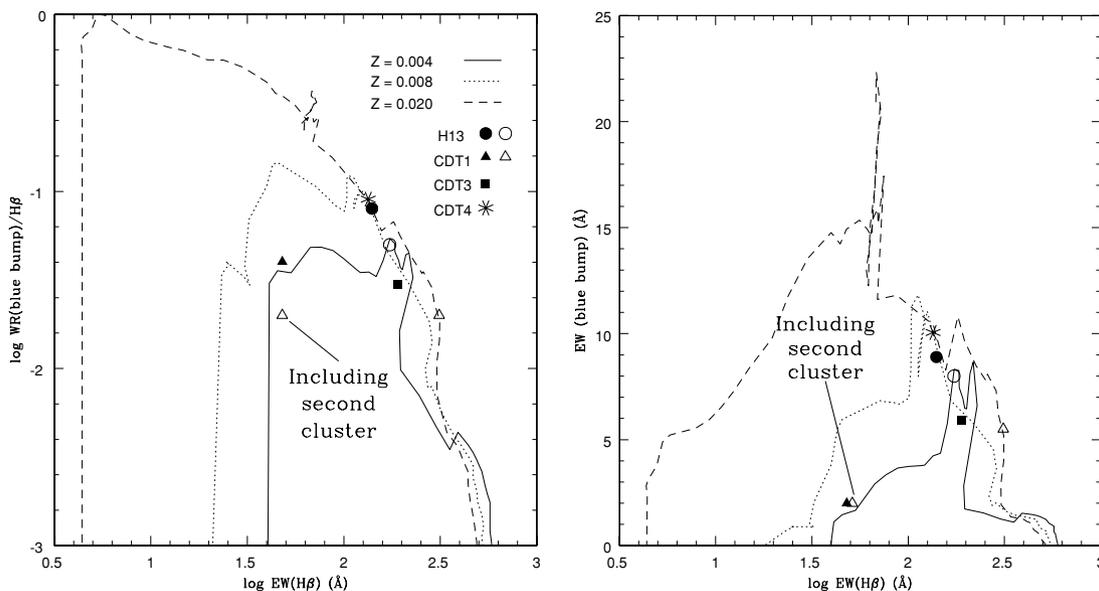

Figure 9. Relative intensity (left) and equivalent width (right) of the WR blue 'bump' versus Hβ equivalent width for SV98 models of three different metallicities as labelled. The data are shown as solid and open symbols as explained in the text.

imperative to interpret correctly the emission line spectra observed in H II regions.

5 SUMMARY AND CONCLUSIONS

We have analysed the stellar populations of 11 H II regions in the galaxies NGC 628, NGC 1232, NGC 925 and NGC 1637 using spectrophotometric observations between 3500 and 9700 Å. We have derived the physical properties of the regions and their corresponding ionizing clusters: filling factor, mass of ionized gas and mass of ionizing stars. Most of the regions have small ionizing clusters with masses in the range 1500 to 30 000 solar masses. The exceptions are the three supergiant H II regions in NGC 1232, CDT1, CDT3 and CDT4 with masses greater than 100 000 solar masses. These values constitute in fact lower limits as the regions are assumed to be ionization bounded and the presence of dust has not been taken into account.

WR features have been observed in the four supergiant H II regions, H13 in NGC 628, and CDT1, CDT3 and CDT4 in NGC 1232. A very detailed modelling has been carried out for these regions by using two different sets of models – those of SV98 for WR star populations and those of Leitherer et al. (1999) for ionizing populations – to try to reproduce both the WR features and the emission line spectrum of each region simultaneously. In all cases, the agreement between both the predicted and the observed values for the WR luminosities and equivalent widths is excellent. This fact seems to indicate that the stellar evolution assumed by the models is predicting the right WR/O ratios at the different metallicities involved.

The ages of the populations containing WR stars are found to be between 2.3 and 4.1 Myr. This population is sufficient to explain the emission line spectrum of the low metallicity region H13 in NGC 628, taking into account the uncertainties involved in both observations and model computations.

This is not the case for the rest of the regions. For CDT1 in NGC 1232, a second ionizing population is required to simultaneously reproduce both the WR features and the emission line spectrum. This second population is older than the previous one by about 5 Myr and contributes about 10 per cent of the ionizing photons and 5 times the continuum luminosity at 9000 Å. Composite populations are also found for half of the regions without WR features, although in this case, the result is based only on the emission line spectrum analysis.

For the other two regions containing WR stars, CDT3 and CDT4 in NGC 1232, no consistent solution is found, since the population containing WR stars produces a spectral energy distribution which is too hard to explain the emission of the gas. Several solutions are proposed to solve this problem. Both a reduction in the number of high energy photons of the ionizing clusters, which could arise naturally with the inclusion of blanketing by metallic lines in the atmospheres of the WR stars, and/or the assumption that the H II regions be matter bounded can effectively solve the problem. The latter hypothesis has been tested successfully (Castellanos et al. 2002) while the former one still remains to be explored.

ACKNOWLEDGMENTS

REFERENCES

Bresolin F., Kennicutt R. C., Garnett D. R., 1999, ApJ, 510, 104
Campbell A., Terlevich R., Melnick J., 1986, MNRAS, 223, 811
Castellanos M., Díaz A. I., Tenorio-Tagle G., 2002, ApJ, 565, L79
Castellanos M., Díaz A. I., Terlevich E., 2002, MNRAS, 329, 315 (Paper I)
Cerviño M., Mas-Hesse J. M., 1994, A&A, 284, 749
Crowther P. A., Pasquali A., de Marco O., Schmutz W., Hillier D. J., de Koter A., 1999, A&A, 350, 1007
Díaz A. I., 1998, Ap&SS, 263, 143
Díaz A. I., Terlevich E., Vilchez J. M., Pagel B. E. J., Edmunds M. G., 1991, MNRAS, 253, 245
Díaz A. I., Castellanos M., Terlevich E., García-Vargas M. L., 2000a, MNRAS, 318, 462 (DCTG00)
Díaz A. I., Álvarez Álvarez M., Terlevich E., Terlevich R., Portal M. S., Aretxaga I., 2000b, MNRAS, 311, 120
Esteban C., Smith L. J., Vilchez J. M., Clegg R. E. S., 1993, A&A, 272, 299
Ferland G. J., 1999, Internal Report, HAZY: A Brief Introduction To CLOUDY. Univ. Kentucky
García-Vargas M. L., Bressan A., Díaz A. I., 1995, A&AS, 112, 13
García-Vargas M. L., González-Delgado R. M., Pérez E., Alloin D., Díaz A. I., Terlevich E., 1997, ApJ, 478, 112
Hodge P. W., 1976, ApJ, 205, 728
Kennicutt R. C., 1983, ApJ, 272, 54
Kennicutt R. C., Hodge P. W., 1980, ApJ, 241, 573
Kurucz R. L., 1992, in Barbuy B., Renzini A., eds, Proc. IAU Symp. 149, The Stellar Populations of Galaxies. Kluwer, Dordrecht, p. 225
Leitherer C., Heckman T. M., 1995, ApJS, 96, 9
Leitherer C., Chapman J. M., Koribalski B., 1997, ApJ, 481, 898
Leitherer C., Schaerer D., Goldader J. D. et al., 1999, ApJS, 123, 3 (STARBURST99)
Lejeune T., Cuisinier F., Buser R., 1997, A&AS, 125, 229
Maeder A., Meynet G., 1994, A&A, 287, 803
Mayya Y. D., Prabhu T. P., 1996, AJ, 111, 1252
Meynet G., Maeder A., Schaller G., Schaerer D., Charbonnel C., 1994, A&AS, 103, 97
Mihalas D., 1972, ApJ, 176, 139
Osterbrock D. E., 1989, Astrophysiscs of Gaseous Nebulae and Active Galactic Nuclei. University Science Books, Mill Valley CA
Pagel B. E. J., Edmunds M. G., Blackwell D. E., Chun M. S., Smith G., 1979, MNRAS, 189, 95
Panagia N., 1973, AJ, 78, 929
Pastoriza M. G., Dottori H. A., Terlevich E., Terlevich R., Díaz A. I., 1993, MNRAS, 260, 177
Pérez E., 1997, MNRAS, 290, 465
Schaerer D., de Koter A., 1997, A&A, 322, 598
Schaerer D., Vacca W. D., 1998, ApJ, 497, 618 (SV98)
Schmutz W., Leitherer C., Gruenwald R., 1992, PASP, 104, 1164
Selman F., Melnick J., Bosch G., Terlevich R., 1999, A&A, 347, 532
Shields J. C., Kennicutt R. C., 1995, ApJ, 454, 807
Smith L. F., 1991, in Haynes R., Milne D., eds, Proc. IAU Symp. 148, The Magellanic Clouds. Kluwer, Dordrecht, p. 267
Vacca W. D., Conti P. S., 1992, ApJ, 401, 5
van Zee L., Salzer J. J., Haynes M. P., O'Donoghue A. A., Balonek T. J., 1998, AJ, 116, 2805
Vílchez J. M., Pagel B. E. J., 1988, MNRAS, 231, 257

This paper has been typeset from a TEX/LATEX file prepared by the author.